The structural, geometric and volumetric changes of a polythermal Arctic glacier during a surge cycle

King, Owen; Hambrey, Michael; Irvine-Fynn, Tristram; Holt, Thomas

Published in:
Earth Surface Processes and Landforms

DOI:
10.1002/esp.3796

Publication date:
2016

Citation for published version (APA):
King, O., Hambrey, M., Irvine-Fynn, T., & Holt, T. (2016). The structural, geometric and volumetric changes of a polythermal Arctic glacier during a surge cycle: Comfortlessbreen, Svalbard. *Earth Surface Processes and Landforms*, *41*(2), 162-177. https://doi.org/10.1002/esp.3796

The structural, geometric and volumetric changes of a polythermal Arctic glacier during a surge cycle: Comfortlessbreen, Svalbard

Journal:	*Earth Surface Processes and Landforms*
Manuscript ID:	ESP-14-0287.R3
Wiley - Manuscript type:	Paper
Date Submitted by the Author:	n/a
Complete List of Authors:	King, Owen; University of Leeds, School of Geography Hambrey, Michael; Aberystwyth University, Department of Geography and Earth Sciences Irvine-Fynn, Tristram; Aberystwyth University, Department of Geography and Earth Sciences Holt, Tom; Aberystwyth University, Department of Geography and Earth Sciences
Keywords:	Surge, Glacier structure, Comfortlessbreen, Geometric changes , Svalbard

The structural, geometric and volumetric changes of a polythermal Arctic glacier during a surge cycle: Comfortlessbreen, Svalbard

Owen KING[1], Michael J. HAMBREY[2], Tristram D.L. IRVINE-FYNN[2], Tom O. HOLT[2]

[1]School of Geography, University of Leeds, Leeds, LS2 9JT, United Kingdom

[2]Centre for Glaciology, Department of Geography and Earth Sciences, Aberystwyth University, Aberystwyth, Ceredigion, SY23 3DB, United Kingdom.

ABSTRACT: Various parameters of the most recent surge of the polythermal glacier Comfortlessbreen in NW Svalbard, have been assessed through a combination of remote sensing and ground observations. Analysis of a digital elevation model time-series shows a marked change in the geometry of the glacier from quiescence (1990 and earlier) into the late surge phase (2009). The transfer of 0.74 km^3 of ice caused up to 80 m of surface drawdown in the reservoir area, above the equilibrium line, whilst ice built up in a spatially concentrated manner in the receiving zone, below the equilibrium line. A ramp of ice, c.100 m above quiescent level, developed in the lower reaches of the glacier late in the surge. Also in the lower reaches of the glacier, structures attributable to the passage of a kinematic wave are identified and the migration of a surge front on the glacier is thus inferred. In a conceptual model, we consider that a bend in the valley, in which the glacier resides, and convergence with tributary glaciers, to be significant factors in the style of surge evolution. Their flow-restrictive interference results in slow initial mass-transfer and the growth of a surge front within 3-4 km of the terminus.

KEY WORDS: Surge, glacier structure, geometric changes, Comfortlessbreen, Svalbard

Introduction

In Arctic latitudes, mountain glaciers and ice caps occupy c. 402000 km^2 (Sharp et al, 2011) of a region subject to recent, rapid warming (Comiso and Hall, 2014). Within some arctic regions, surge-type glaciers are abundant, with particular prevalence in areas of Alaska and Svalbard (Sharp et al 2011). While the occurrence of surging is not necessarily related to a changing climate, such environmental dynamics can alter surge frequency (Dowdeswell et al., 1991; Eisen et al., 2001; Dowdeswell et al., 1995; Frappê and Clarke 2007; Copland et al., 2011; Sharp et al 2011). However, the geographical and temporal variability of surge behaviour has resulted in an inadequate understanding of the processes and products of glacier surges. Consequently, the aims of this paper are to evaluate the structural, geometric and volumetric changes of a typical polythermal valley glacier in Svalbard during a recent surge, to compare these changes with other surge-type glaciers in the region, and to develop a conceptual model of surge evolution.

Typically, surge-type glaciers experience cyclical velocity fluctuations, whereby short periods of increased flow (1-15 years) and mass-displacement punctuate longer periods (lasting decades to centuries) of quiescence and ice build-up (Raymond, 1987; Murray *et al.*, 2003a). The duration of each component of the surge cycle varies between different clusters of surge-type glaciers around the world. In polythermal glaciers of Svalbard, the active phase of a surge, typically lasts 3-15 years, whereas temperate surge-type glaciers in other regions, such as in Alaska, typically surge for 1-2 years (Jiskoot *et al.,* 2000). The quiescent phase of Svalbard glaciers typically lasts 50 years or more, with a period of 12-20 years more typical of Alaskan surge-type glaciers (Eisen *et al*., 2005, Bevington and Copland, 2014). Surge-phase velocities are 10-1000 times greater than quiescent-phase flow (Meier and Post, 1969; Murray *et al*., 2003b), whereas quiescent-phase flow is lower than the balance velocity of the glacier (Mansell *et al*., 2012). The slowdown of a glacier following its surge can take years in Svalbard (Mansell *et al*., 2012), whereas in Alaska a surge may terminate in days or weeks (Murray *et al.,* 2003b). Less than 1% of the world's glaciers are thought to be of surge-type (Murray *et al.*, 2000) but, where situated, their distribution is markedly non-uniform, with pronounced clustering on a global and regional scale (Jiskoot *et al.*, 2000). A substantial concentration of surge-type glaciers is present in Svalbard, an archipelago containing ~36,000 km^2 of glaciers and ice caps spread over four main islands (Hagen *et al.*, 1993; Dowdeswell and Hambrey, 2002). Estimates of the proportion of surge-type glaciers in the total glacier population of Svalbard vary enormously, ranging from 13 % (Jiskoot *et al.*, 1998) to 90 % (Lefauconnier and Hagen, 1991).

A conclusive understanding of the mechanism(s) of, and disparities associated with, surge initiation, development and termination remains elusive. Various hypotheses have been presented to explain the phenomenon across different clusters of surge-type glaciers (e.g. Clarke, 1976; Kamb, 1987; Fowler *et al.*, 2001; Nolan, 2003). A hydrological switching model is suggested to be most applicable to surge-type glaciers in coastal regions of Alaska, based on intensive research on Variegated Glacier. The model is based around the concept that surge initiation and termination occur in response to a switch in the efficiency and configuration of a basal drainage system (Kamb *et al.,* 1987; Eisen *et al*., 2005). The surge trigger in this model may be the point at which a subglacial till layer fails at some critical basal shear stress, in response to significant water penetration sourced englacially. Soft-bed deformation over a wide area would then promote surge-type flow. Surge termination would occur through a progressive decrease of the basal shear stress and a sudden and large increase in water-flux, re-establishing a more efficient subglacial drainage system (Eisen *et al*., 2005). In contrast, the thermal-switch model, developed initially by Clarke (1976) and Clarke *et al.* (1984) for Trapridge Glacier, Canada, and elaborated by Fowler *et al.* (2001) is often considered most applicable (although not exclusively) to Svalbard's surge-type glaciers. In the model's simplest form, Fowler *et al.* (2001) suggested that surge-type behaviour might be a result of the evolving thermal regime at the glacier bed. In such a model, the evolutionary morphology of a surge to some degree is tempered by the behaviour of an activation-wave (the area of thermal switch), which travels through the glacier system. This activation-wave may propagate at various rates with an inconsistent path; thus a spectrum of surge styles develops. Murray *et al*. (2012) distinguished two different styles of surge development in Svalbard depending on where this activation wave may originate. In land-terminating surge-type glaciers, such as Bakaninbreen, fast flow appears to begin in the reservoir zone of the glacier and migrates downglacier. In tidewater glaciers, fast flow appears to initiate lower down on the glacier and spreads both up and down-glacier (e.g. Monacobreen: see Murray *et al.,* 2003b).

In this study, we examine the behaviour of Comfortlessbreen (Figure 1), a surge-type glacier in northwest Spitsbergen, during the active phase of its most recent surge cycle, which took place between 2006 and 2010. Digital elevation models (DEMs) of the glacier surface are generated, and aerial photographs prior to and during the surge cycle are studied to decipher the geometric, volumetric and structural changes at the glacier's surface. These remote-sensing analyses are complemented by prior geomorphological observations in the early 1990s, during quiescence, and a rapid reconnaissance of the glacier margin in 2009, just prior to surge termination. Combined, these results enable the formulation of a conceptual model of Comfortlessbreen’s recent surge, which seeks to augment the existing knowledge-base relating to the mechanics of glacier surging.

Study site

Comfortlessbreen (78°45’42”N, 12°9’36” E) in NW Spitsbergen is a valley glacier that is c. 15 km in length, has an area of 64.7 km^2 (including tributaries) and an estimated volume of 11 km^3 (Hagen *et al.*, 1993). Approximately 2.5 km wide, the glacier initially flows WNW where it is fed by several cirque glaciers (Figure 1), before gradually making a broad 45° turn to the NNW at half its length. It is confluent with two smaller valley glaciers, Nordenfjeldskebreen and Smalfjellbreen, and the combined flow units enter Engelskbukta (“English Bay”), terminating as an incipient piedmont lobe, 3.3 km wide, both in tidewater and on an alluvial plain underlain by dead glacier ice. Geophysical surveys in 1978-1979 reported ice depths between 308 and 400 m for the lower 10 km of the glacier tongue, excluding the lowermost 1.5 km (Kotlyakov and Macheret, 1987).

The glacier forefield is dominated by a large terminal thrust-moraine complex that is assumed to mark its Neoglacial and mid-Holocene limits (Huddart and Hambrey, 1996). When Comfortlessbreen advanced to this position, it joined Uvêrsbreen, collectively producing this thrust-moraine complex. As the combined glacier receded, extensive dead-ice areas became buried under an active braid-plain and major channel switching took place several times, eroding parts of both moraine complexes. The geomorphology of the proglacial area in mid-surge illustrates the relationship between the glacier, braid-plain and moraine complex (Figure 2), and this also has a bearing on understanding past glacier dynamics (Figure 2). Norsk Polarinstitutt aerial photographs from 1936 (oblique), 1956, 1977 and 1990 respectively (illustrated in Brand *et al.*, 2007) emphasise the retreat of the glacier throughout this period.

Until the current surge, Comfortlessbreen showed few signs of former surge-type behaviour, such as contorted (looped) moraines, potholes and stagnant ice (Post and La Chapelle, 1971). Croot (1988) suggested that Comfortlessbreen was a surge-type glacier on the basis of well-developed folded moraines at the eastern margin, but these are better interpreted as the product of longitudinal compressive flow as the glacier spreads out into its forefield (Figure 2). Furthermore, the glacier’s Neoglacial moraine complex is insufficiently distinctive to be attributed to a surge origin. Rather, Comfortlessbreen seemed to be typical of a slow-flowing glacier with a well-developed dendritic drainage network and few crevasses, except close to the then-calving front. Indeed, Jiskoot *et al*. (2000) removed the glacier from earlier lists of surge-type glaciers in the absence of surge data.

Interpretation of aerial photographs and ASTER imagery shows that the glacier underwent c. 250 m of recession between 1990 and 2002, after which the glacier began to show the first signs of reactivation. From 2002 to 2004 part of the glacier front advanced 100 m into the sea. Full-scale surging was evident by 2006 (Sund *et al.*, 2009). Between 2002 and 2009 the front advanced 500-700 m and the terrestrially based lobe was reactivated across the whole front during 2009 (Sund and Eiken, 2010) (Figure 3). Evidence of ice-push phenomena, including deformation of the permafrost on land and bulldozing of marine sediments, was observed in June 2008, and by July 2009 these processes were active along much of the ice front. The resulting push moraine effectively separated the glacier terminus from direct contact with tidewater. Major changes also occurred in the proglacial area with the main water discharge from the NE margin of Comfortlessbreen, combined with that from Uvêrsbreen, becoming diverted across the front of the glacier, rather than towards the glacier forefield. The proglacial braidplain also began collapsing into a recently formed lagoon. The surge terminated in 2010 (Mansell *et al.*, 2012).

Previous work on Comfortlessbreen has attempted to categorise stages of surge development (Sund *et al.*, 2009), to quantify surface velocities during quiescence and at various points through the surge phase (Mansell *et al.*, 2012; Schneevoight *et al.*, 2012), and to derive ice surface build-up during quiescence (Nuth *et al.*, 2007). To our knowledge, no work has been undertaken with the aim of assessing the structural state of the glacier at any point, or to assess the geometrical changes experienced during surge. These parameters are important when considering the style of and mechanisms responsible for surge initiation and development.

Methods

The surge of Comfortlessbreen is examined primarily through the analysis of remotely sensed datasets, supplemented by field observations made during the surge in July 2009. The primary data source of data used was the Norsk Polarinstitutt's archive of vertical aerial photography (table 1), from which three sets of digital and scanned scenes were obtained providing complete coverage of the study area for summers 1990, 2008 and 2009. The imagery is of sufficient overlap and resolution (1 m and 0.4 m per pixel for 1990 and 2008/9 imagery respectively) to allow for both the photogrammetric extraction of topographical data and the clear identification and digitisation of all significant structural features present at the surface of the glacier. A subset of the Norsk Polarinstitutt's 1990 DEM of Svalbard was also acquired to allow for dataset comparison and accuracy derivation. This dataset has a grid-cell size of 20 m, and an estimated vertical accuracy of ~±2 m RMS for gently sloping terrain and ~±6 m over steeper topography (Sund *et al.*, 2009).

Structural identification and mapping

Glacier structures were mapped across all three sets of imagery through hand-digitising features as polygons and polylines in ESRI ArcMap Geographical Information System (GIS, Version 9.3). The structures were mapped at a maximum resolution of 1:5000 to retain image detail, but still allow the identification of individual features. Structures mapped included crevasses, crevasse traces, snow-bridged crevasses, longitudinal foliation and folding. Structures were identified and categorised according to a set of criteria used in aerial photography and satellite imagery, which have been developed from structural studies on surge-type glaciers (e.g. Hambrey and Dowdeswell, 1997; Glasser *et al.*, 1998; Grant et al., 2009), temperate valley glaciers (e.g. Hambrey and Lawson, 2000; Goodsell *et al.*, 2005; Jennings et al. 2014) and ice shelves (e.g. Glasser and Scambos, 2008; Holt *et al.*, 2013). Structural attributes, for example crevasse azimuth, were extracted and quantified using the geometric calculator in ArcMap and GEOrient software. Geomorphological mapping of the immediate proglacial area was achieved by enhancing an existing map (Huddart and Hambrey, 1996) using a Quickbird satellite image from 28 August 2008.

DEM extraction

DEM extraction was undertaken using ENVI software (version 5.1) and its multi-stage DEM extraction wizard (for details see ENVI, 2009). Following the guidelines of studies such as James *et al.* (2012) and Barrand *et al.* (2009), particular care was taken during the image-matching stage, as a significant source of DEM error may arise through a poor relation between imagery and the ground-coordinate system. At least 35 ground-control points (GCPs) and 75 tie points were collected for each image pair to ensure constrained correspondence of left and right epipolar images before the extraction of elevation data. GCPs were selected with the aid of the Norsk Polarinstitutt's Topo-Svalbard online map resource (http://toposvalbard.npolar.no/) and comprised distinctive, stable land surfaces and easily identifiable spot heights. Following the derivation of elevation (z) data, surface construction was achieved through the use of a Delauney triangulation gridding algorithm, a method of interpolation often used in glaciological, DEM-based studies (e.g. Kohler *et al.*, 2007; Nuth *et al.*, 2010). DEM-extraction parameters, such as moving window size, were variably set during DEM-geocoding, but each DEM was resampled to a 10 m grid before analysis.

Secondary interpolation was undertaken over some small areas to re-build the glacier surface to a similar topography as the surrounding ice. This was necessary in areas of poor optical contrast (where snow cover or dark shadow predominated in different scenes) where DEM quality was unsatisfactory. It was possible to obtain DEM coverage of the glacier and its surrounding topography from 1990 and 2009 imagery, with DEMs of the lower two-thirds of the glacier extracted from 2008 scenes.

DEM quality assessment and accuracy

The quality and accuracy of extracted DEMs was assessed using a two-stage approach. First, the quality of image-bundle adjustment was assessed through the derivation of root mean-squared error (RMSE in X, Y and Z coordinates) for ground-control points. Over the three DEM sets, average RMSE values of ground-control points in X, Y and Z were 2.72, 2.85 and 2.81 m respectively. These figures suggest a good match between stereo-image pairs and ground-coordinate systems. Second, DEMs were compared with an independent dataset of known accuracy to allow an estimation of surface accuracy. The 1990 DEM set extracted in this study was differenced with the NPI's 1990 DEM to allow quantification of surface similarity. The mean deviation, standard deviation and relative standard deviation between the two datasets are 9.1 m, 15.8 m and 1.73% RSD respectively.

Such an approach was not possible for the 2008 and 2009 DEM sets as a source of appropriate, comparable datasets could not be located. The low RMSE values through all DEM sets suggests consistently well constrained elevation data in relation to the ground-coordinate system; thus similar accuracy estimates would be expected for 2008 and 2009 DEMs, particularly where good surface conditions existed for DEM extraction.

Volume change

The derivation of volume change between 1990 and 2009 was achieved following the simple method of Hagen (1987). As ice-surface elevation change was known (following differencing), volume change could be calculated through the multiplication of this pixel value with pixel area. Volume change values were then summed in zones above and below the equilibrium line altitude (ELA) to yield ice transfer values from reservoir to receiving zones.

Structural glaciology

Previous structural analyses of surge-type glaciers, leading to the derivation of polyphase deformation histories during both quiescent and surge phases, are the result of detailed field surveys (e.g. Lawson *et al.*, 1994; Hambrey and Dowdeswell, 1997). Such complex observations have not been made here, as heavy crevassing precluded ready access to the glacier surface. Nevertheless, structural mapping allows the documentation of the occurrence of a suite of structures at the surface of the glacier, providing the basis for an understanding of the variable stress and strain regime through the glacier system over time.

Quiescent state structures (1990)

Aside from minor crevassing around topographical obstacles and headwalls in tributary cirques, the ice surface of the reservoir zone shows limited evidence of surface disturbance in 1990 imagery (Figure 4). Where the valley narrows, and tributary flow units converge into the main glacier tongue, three main surface traces become apparent (Figure 5a). Firstly, there are numerous longitudinal flow-parallel foliae, which alternate between dark and light ice along the eastern edge of the glacier's main flow unit (at the Smalfjellbreen confluence), and along its western flank. These features are of considerable length (1-4 km) and are clearest where flow units coalesce and debris emphasises their trace. Secondly, and more towards the glacier's centreline, a set of evenly spaced (~75 m) crevasse traces occur as thin, dark surface features showing a generally similar orientation. These traces have a concordantly evolving orientation down-glacier, beginning as transverse features and rotating to become arcuate (concave down-glacier) towards the Nordenfjeldskebreen confluence. A set of more evenly spaced and arcuate crevasse traces occurs on the grounded portion of the glacier's terminus. A further set of diffuse light and dark layering can be seen in the main glacier tongue within approximately 3 km of the glacier's terminus. These are distinguishable from the crevasse traces described above because of their variable orientation and inconsistent surface trace, and have thus been identified as remnant primary stratification. Additionally, note should be made of the deformation of the medial moraine separating the main Comfortlessbreen/Smallfjellbreen flow unit and the Nordenfjeldskebreen unit. This feature develops as the main glacier tongue expands into a piedmont-style lobe towards Engelskbukta and longitudinal compression intensifies.

Significant fracturing of the ice surface is restricted to the calving zone of the glacier. Here, extensive transverse, arcuate (convex down-glacier) crevassing is evident across the tidewater-terminating portion of the glacier. These extend approximately 2.5 km up-glacier and intersect the longitudinal surface traces described above. A result of this limited fracturing is a well-developed dendritic supraglacial drainage network, which extends into the reservoir zone towards the cirques at the head of the valley (Figure 1).

Structural developments early in the surge phase (2006-2008)

In the reservoir zone, an extensive crevasse network dominates the glacier surface by 2008 (Figure 4). This crevassing is almost exclusively transverse (and thus NE-SW-orientated; Figure 6), but rotates towards a more arcuate pattern at the glacier margins. At these margins, especially along the true right of the valley (Figure 1 and 4), a narrow (200-300 m) zone of chaotic crevassing is evident. Such a crevasse network is consistent to slightly below the equilibrium line, from where its pattern and density alters. Down-glacier of the Smalfjellbreen confluence, more longitudinally orientated crevasses splay towards the glacier margins, and there are large areas where the ice-surface is undisturbed near the glacier centreline. At the terminal zone of the glacier, a chaotic blocky crevasse pattern replaces the concave crevassing of late quiescence. Again, longitudinal, splaying crevasses emanate from the glacier centre, intersecting a set of transverse fractures up to 750 m from the glacier front.

In addition to the widespread surface fracturing that occurred during the early stages of the surge, notable evolution of pre-existing surface features occurred between 1990 and 2008. The longitudinal foliation that was so evident during late quiescence displays a more limited coverage late in the surge, although these deep-seated structures cannot have been destroyed completely; their surface expression is hidden as a result of surface disturbance by crevassing. Foliation was limited to the area down-glacier of the Nordenfjeldskebreen confluence. In areas formerly dominated by longitudinal foliation, a few large “isoclinal” and “similar” fold features can now be identified. These features have limbs a few hundreds of metres in length and axes aligned parallel to flow. Lastly, an extensive set of transverse uniform crevasse traces developed to mirror the crevasse pattern of 1990 within approximately 2.5 km of the glacier front.

Late surge phase structural change (2008-2009)

Apart from a denser distribution and greater number of crevasses, the pattern present in the reservoir zone of the glacier in 2009 essentially mirrors that of early stages of the surge (Figure 4). Below the equilibrium line, however, significant structural changes occurred between 2008 and 2009. Fracturing of the glacier surface intensified during this later surge stage, and an extensive, chaotic crevasse network is present within 1 km of the glacier front in 2009 imagery. There are broad areas of variably orientated but intersecting longitudinal and transverse crevasses (Figure 5), and little of the ice surface remains undisturbed in this area.

Intertwined with this chaotic surface-fracturing, fold features are once again in evidence (Figure 5). These folds now spread across the glacier’s width, and have limbs up to 1 km in length. Their axes remain aligned parallel to flow, and they are tight and in some cases isoclinal; again they are dominant where the clearest examples of longitudinal foliation occurred. Of interest is the clarity of longitudinal surface traces further up-glacier at this late stage of the surge, with pronounced examples evident along several kilometres of the glacier's western margin.

The network of crevasse traces, which took up the 1990 crevasse pattern in 2008, is much diminished in 2009 imagery. Few crevasses remain close to the glacier front, nor further up the glacier system.

Late surge-phase ground observations (2009)

Access to the western (true left) margin of Comfortlessbreen in July 2009 allowed inspection of on-going ice deformation and highlighted the importance of debris-transfer processes, as well as revealing ice-marginal structures exposed in vertical faces not visible in aerial photography. A prominent shear zone comprising chaotic crevasses and séracs up to several metres high marked the marginal zone. There were also extensive drapes of debris on inter-crevasse blocks (Figure 7a). Two main sedimentary facies were identified at the left-lateral margin that illustrated the nature of ice-marginal structural evolution, in effect the last structures to be produced as ice is transferred through the glacier:

(i) Clast-rich muddy diamicton, comprising >40% clasts grading into muddy gravel with c. 60% clasts. Subrounded clasts are dominant. This facies, prior to its entrainment, is interpreted as basal till.

(ii) Sandy gravel, comprising c. 60% clasts that are predominantly sub-rounded and sub-angular. This is the same material that occurs on the inner slopes of the Neoglacial lateral moraines, indicating ice-marginal reworking of this material.

The dominant mechanism for entrainment of these facies is thrusting, wedges of sediment 2-3 m thick being evident at the glacier base (Figure 7b), and discrete layers at higher levels in the glacier, especially towards the western margin (Figure 7c). A mechanism commonly attributed to surging glaciers, but rarely observed, is the filling of basal crevasses (e.g. Woodward *et al.*, 2002), but only one example of such a crevasse was observed (Figure 7d). Deformation was transmitted about 10 m beyond the ice margin in a few places, with the buckling of snow banks being the most obvious manifestation of this (Figure 7e).

A third sedimentary facies is glaciomarine mud, derived from the shallow bottom of the bay to form a ramp in front of the advancing cliff, by "bulldozing" of the sea floor. The style of deformation here was different from that occurring on land. It was characterised by a series of gently curving ridges a few metres high and tens of metres long (as many as five ridges, sub-parallel to the ice margin), as evident in the most advanced part of the glacier (Figure 7f). A single ramp-and-ridge complex of glaciomarine sediment separated the glacier from tidewater meaning that the glacier was no longer strictly terminating in tidewater in 2009, in contrast to its pre-surge state.

Geometrical changes

Ice surface profile evolution and differenced DEMs

Longitudinal elevation profiles of the glacier surface, taken along the centre-line of derived DEMs, are illustrated in Figure 8, and the results of 1990-2009 DEM differencing are shown in Figure 9. They display significant evolution of the ice-surface profile, from quiescence into the later stages of the surge. In 1990, the profile of the glacier surface was distinctly linear and its gradient uniform. By 2008, a significant rearrangement of the glacier surface had occurred, with a large-scale increase of ice-surface elevation over much of the receiving zone, and a gently graded bulge developing over most of this area. Above the equilibrium line, despite limited DEM coverage, ice-drawdown can also be observed. Between 1990 and 2008, the maximum vertical thickening of the surface was 80 m. This occurred 5 km from the glacier terminus, around the area of the Smalfjellbreen confluence. Between 2008 and 2009, as with those structural changes described above, major geometric changes occurred in the lowermost portion of the glacier. The general inflation of the ice surface of the previous year had become spatially concentrated in 2009, with a steeper-sided (15-20^{o}), glacier-wide front developing within approximately 3 km of the glacier terminus (Figure 9). This mass of ice appears to have developed independently of other ice below the equilibrium line. Ice-surface elevation decrease (of between 20 and 60 m) is documented further up-glacier between 2008 and 2009, despite this area of the glacier still being below the equilibrium line. The peak increase of ice-surface elevation between 1990 and 2009 reached 100 m or more where this large ramp developed. This 2009 ice-surface profile also shows a drawdown of ice from the reservoir zone, with ice levels 80 m or more below the 1990 surface furthest up-glacier. DEM-differencing high up in the glacier system is suggestive of 100 m or more of ice-surface drawdown, but with poor optical contrast in 2009 imagery, the reliability of these results should be considered cautiously.

Volume change

Between 1990 and 2009, the reservoir and receiving zones experienced ice losses of 0.74 km^3 and gains of 0.80 km^3, respectively. Volume-change data have not been gathered from the 2008 DEM because of incomplete coverage. It should be noted that some areas of the 2009 DEM, covering the highest reaches of the reservoir zone, were excluded from this analysis because of poor optical contrast in the imagery and resultant poor DEM quality. As this is the area of the glacier where most ice-surface elevation decrease was seen, the total calculated volume of ice lost from the reservoir zone should be considered an underestimate, with an actual figure likely to be much greater had DEM coverage been complete. Indeed, these figures also fail to account for any mass lost through ablation during the surge, suggesting that a true figure of ice-gain in the receiving zone would be higher than has been derived through DEM-differencing.

Discussion

Stress and strain regime inferences from structural features

Herzfeld *et al.* (2004) referred to crevasse patterns as 'the writings in a glacier's history book', that is, they present the clearest record of the movement, strain and deformation in ice over a certain time-span. The analysis of crevasse patterns present at the surface of a glacier therefore allows inferences about the recent ice-dynamic processes that the glacier has experienced. The orientation of crevasses is normally dependent on the direction of maximum extending strain-rates, with a fracture typically forming perpendicular to the maximum extending strain-rate (Cuffey and Paterson, 2010). A simple approach is to identify similar crevasses sets or classes, make inferences about the dynamic regime they represent, and to then collate the information of each crevasse class to derive a composite representation of past flow regime. This approach is taken below, with distinct crevasse belts identified in imagery over the three years of study and their relation to the stress and strain regime experienced at the glacier surface discussed accordingly. Further to this, consideration of the cumulative strain history of certain features is also made, as the form of structures such as foliation and folds is largely dependent upon the variable deformation of ice as it moves through the glacier system, or is subject to different phases of deformation (Hambrey and Dowdeswell, 1997; Hambrey and Lawson, 2000).

Pre-surge evolution

The pervasive presence of longitudinal foliation at the glacier surface in the ablation zone in 1990 suggests lateral compression as the predominant component in the deformational history of ice passing through the glacier system during quiescence. Longitudinal foliation is believed to form through the folding and transposition of primary layering as ice, from a single flow unit or more, converges from a wide accumulation zone into a narrower glacier tongue. Comparable foliations have been observed in a number of non-surge type glaciers and some surge-type glaciers in their quiescent phase. The prominence of foliation close to the margins of Comfortlessbreen and its main flow units (Figure 4) is a result of the concentration of folding and simple shear in these zones (Lawson *et al.*, 1994; Hambrey and Lawson, 2000), particularly where the main flow unit is joined by tributary glaciers. The evolving orientation of crevasse traces close to the centreline of the glacier shows differential flow between the middle of the glacier and its margins. Such curved or arcuate features have been described in detail by Lawson *et al.* (1994), and are attributable to creep-dominated flow. Longitudinally compressive stresses are confined to the portion of the glacier tongue that expands into a piedmont-style lobe towards Engelskbukta. The folded medial moraine showcases this style of deformation.

Active fracturing of the glacier surface was restricted to, and associated with, the calving portion of the glacier terminus in 1990 (Figure 5). The longitudinal extension promoted by the reduced basal friction of this terminal area is the only evidence of more active flow at this point in quiescence. Blaszczyk *et al.* (2009) measured the length of the crevassed zone from the glacier terminus in 2001, and estimate 350 m of ice fracturing from the ice front up-glacier. From our 1990 mapping, this zone of crevassing was formerly up to 1 km in length. With continued recession of the glacier terminus before surging began, the terminus probably became more grounded, although the fractured ice surface would have remained because of the previously extensional flow. A similar pattern of crevassing has been described on Perseibreen, Svalbard, during pre-surge retreat (Dowdeswell and Benham, 2003).

Structural evolution during the surge

The extensive crevasse network present in the reservoir zone of the glacier and its tributary cirques in 2008 (Figure 4) indicates increased flow and disturbance of the ice surface into the surge phase. The transverse arrangement of these crevasses indicates a longitudinally extensive flow regime, with flow moderated closer to the glacier margins where crevasses rotate slightly as a result of drag at the valley sides. The ridges of chaotic crevassing at the margins of the glacier are inferred as shear zones formed by the *en masse* block-like flow common during the active phase of a surge (Sund and Eiken, 2010). Such flow has previously been identified by Mansell *et al.* (2012) along much of the length of Comfortlessbreen. The lack of compressive flow features in the reservoir zone (Figure 4) indicates that ice was being drawn down and away from this area, rather than being pushed through the glacier system from the head of the valley. This mechanism contrasts with the case of Bakaninbreen, where a prominent bulge associated with thrusting developed and moved down-glacier, although not the full distance to the terminus (Hambrey *et al.*, 1996; Murray et al., 1997). Down-glacier of the Smalfjellbreen confluence, longitudinally orientated crevasses indicated longitudinally compressive flow, along with crevasses that splayed towards the valley sides (Figure 5). These are imprinted on more transverse crevasses. Collectively, these structures show how ice, which was being transferred from the reservoir zone, was subject to a number of different deformation phases before reaching this point lower in the glacier system. This is in contrast to a parcel of ice taking the same route during quiescence when flow and deformation rates were low.

The modification of quiescent-phase structures also provides evidence of the surge-phase stress and strain regime. Features such as foliation and large-scale folding are the product of cumulative strain, with their form or intensity modified by longitudinal compression and simple shear at flow-unit margins of contrasting velocity (Allen *et al.*, 1960; Hooke and Huddleston, 1978; Hambrey and Lawson, 2000). The scale of folding and the clarity of foliae, despite widespread surface disintegration (Figure 5), emphasises the preservation of quiescent-phase deformation features.

Continuing into 2009, the intensification of crevassing in the reservoir zone indicates the continued drawdown and extraction of ice from this area, as does the development of more extensive shear margins. The development of longitudinal splaying and chaotic crevasse sets in the receiving zone of the glacier reinforces the view of mass-transfer induced by compressional flow.

Arguably the most important structural development in this zone of the glacier is the reduced number and distribution of crevasse traces between 2008 and 2009 (Figure 5). Crevasse traces present structural weaknesses in ice (Hambrey and Lawson, 2000), which are prone to re-activation, often through faulting (Hambrey and Müller, 1978; Hambrey *et al.*, 1999), when subject to longitudinal compression. Such faulting also introduces an element of vertical extension to the deformational history of glacier ice. Murray *et al.* (1998) described how a surge, including the passage of a pronounced front, travelling as a kinematic wave, often leads to the vertical extension of more stagnant glacier ice, along with the intense longitudinal compression of ice in its path. Thus compressional features, such as surface folds and longitudinal-splaying crevasse patterns, along with evidence suggestive of faulting near the terminus (from field observations and a diminishing number of crevasse traces), represent the structural signature of such a phase of deformation and therefore the passage of a surge front on Comfortlessbreen. The propagation of surge fronts on glaciers such as Bakaninbreen (Hambrey *et al.*, 1996; Murray *et al.*, 1998) or Trapridge Glacier (Frappé and

Clarke, 2007), for example, were also accompanied by a significant geometric change at the glacier surface and marked changes in surface velocity. Such parameters must therefore be considered to support the inference of surge front propagation, currently based solely on structural interpretations.

Structure distribution and channel geometry

A significant observation to be drawn from the distribution of those surge-phase structures described above is the coincidence of the zone of transition from extensional to compressive flow in the glacier system, indicated by surge phase structures, and the marked change in channel geometry at approximately half the valley's length. Up-glacier of the bend in the valley and the Smalfjellbreen confluence, where the main flow unit is relatively straight and of constant width (2.5 km), surge-phase structures are indicative exclusively of longitudinally extensional flow. Where the valley bends and narrows to 1.8 km, and tributaries coalesce, compressive features begin to predominate. This clear transition indicates that the change in channel geometry is important in assessing the bulk dynamics of the glacier, and therefore the likely evolution of the surge. Similar relationships have been observed in simulations of the influence of variable channel width and lateral drag (e.g. Pimentel *et al.*, 2010; Adhikari and Marshall, 2012) on glacier flow, with channel-narrowing shown to have a negative effect on glacier flow.

Thus the bend of the valley in which the glacier is located, together with interference from the Smallfjellbreen and Nordenfjeldskebreenflow flow units, restrict the flow of the glacier, resulting in longitudinally compressive flow. This constriction to ice flow would have presented a considerable barrier to a sudden, large-scale mass transfer at the beginning of a surge.

Comparable geometrical changes

Table 2 provides a comparison of the geometrical changes seen on various glaciers through their respective surge phases. The amounts of surface-lowering and ice-thickening over different areas of Comfortlessbreen are similar to those identified in previous studies. The height of the suspected surge front is also similar in scale to those observed on Bakaninbreen and Finsterwalderbreen in Svalbard, and Variegated Glacier in Alaska (Raymond, 1987; Murray *et al.* 1998; Hodgkins *et al.* 2007). There appears to be sufficient structural evidence, namely compressional features such as thrust-faults, folded foliation and longitudinal/splaying crevasses, and geometrical similarities with previous reported examples, to infer that the surge of Comfortlessbreen was manifested as a pronounced front.

Ice dynamics at Comfortlessbreen

As noted above, several studies have been undertaken with a focus on assessing various parameters of Comfortlessbreen's most recent surge. In regard to ice dynamics, studies have focused on both the early and later stages of the surge, and can be summarised as follows:

(1) *Surge initiation*: Sund *et al.* (2009) defined the beginning of the Comfortlessbreen surge as 2006. Prior to this, significant ice-surface build-up (60-80 m) occurred in the upper reaches of the glacier between 1936 and 1990 whilst the glacier front continued to recede (Nuth *et al.*, 2007). From aerial photographs and ASTER imagery, the glacier front receded c. 250 m between 1990 and 2002. From 2002 to 2004 the first signs of activation of the terminus were evident as the glacier advanced 100 m into the sea, prior to the full-scale surging evident from 2006 onwards (Sund *et al.*, 2009). Schneevoight *et al.* (2012) presented a velocity field derived for Comfortlessbreen from 1996 ERS-1/-2 radar data. Their results reflect the flow regime suggested by the crevasses present at the glacier surface in 1996, with a zone of increased ice velocity (0.18 m d^{-1} or ~65 m a^{-1}) at the calving front extending slightly up-glacier. Velocities over the rest of the glacier were appreciably lower, with the lowest (0.03 m d^{-1} or ~11 m a^{-1}) being restricted to an area adjacent to the ridgeline separating Smalfjellbreen and the main glacier tongue, and where Smalfjellbreen and Comfortlessbreen coalesced. Away from this area, flow rates were higher and generally uniform, other than towards the calving front. This flow field offers support to the hypothesis that this segment of the glacier system is important in its bulk dynamics, with increased lateral drag and transverse compression potentially tempering flow around the equilibrium line. Blaszczyk *et al.* (2009) also calculated glacier velocities close to the terminus through feature tracking on ASTER scenes. They estimated flow rates of 55 m a^{-1} over this part of the glacier. Comparison of values estimated by Schneevoight *et al.* (2012) and Blaszczyk *et al.* (2009) indicates a slowdown in ice flow towards the terminus of the glacier during quiescence.

(2) *Surge phase:* The velocity time-series presented by Mansell *et al.* (2012) indicates that surface-velocity maxima coincided with the years in which evolution of the ice-surface profile was most significant. This time-series shows a sharp increase in surface velocity in 2008, leading to a peak in 2009, with a maximum of 1.95 ± 0.25 m d^{-1}. These velocities are similar to those of Sund and Eiken (2010) who recorded a monthly average reading of 2.0 m d^{-1}

along almost the entirety of the glacier late in 2008. This phase was preceded by sporadic but less significant increases in velocity (up to 0.6 m d^{-1}) from 2005/2006. The surge phase was accompanied by dramatic changes in the proglacial geomorphology, with evidence of ice-push phenomena (including deformation of the permafrost and bulldozing of marine sediments at the ice margin), switching of the main water-discharge route from true right to true left side, and collapse of the alluvial plain that covered dead glacier ice into a newly formed lagoon. Surge termination was indicated by a rapid return to values close to those measured by Schneevoigt *et al.* (2012) (0.2 m d^{-1} or less). This time-series subsequently suggests an active surge-phase length of 3-4 years for Comfortlessbreen, similar to or shorter than, those recorded in other Svalbard glaciers (Murray *et al*. 2003b).

Changes in subglacial conditions

Little is known of the characteristics of the bed beneath Comfortlessbreen. The glacier is assumed to be a mostly-temperate polythermal glacier, with geophysical evidence of centreline ice thickness exceeding 300m for at least 60% of the glacier's length, coupled with internal reflection horizons caused by increased interstitial water content at depths of 102-154m, implying a transition from cold surface to temperate englacial and basal ice (Kotlyakov and Macheret, 1987). This inferred thermal regime resembles that of the nearby, similarly large, glaciers Uvêrsbreen (Bjornsson *et al.*, 1996) and Kongsvegen (Hagen and Sætrang 1991). The bed reflection reported for Comfortlessbreen was more coherent than for many other similarly thick, surging glaciers (e.g. Nathorstbreen and Monacobreen: Kotlyakov and Macheret, 1987). Whilst temperate, wet-bed conditions can enhance the reflection at the glacier-bed interface that is identified in geophysical surveys (Bamber, 1989), the specific geology of the Comfortlessbreen catchment may also contribute to this observation. The mountains on either side of the glacier comprise a sequence of Neoproterozoic metamorphosed tillite, psammite and pelite, whilst a rib of marble (dielectric constant 8-13) runs orthogonally from the middle of the terminus (Hambrey and Waddams, 1981; Harland *et al.*, 1993; Harland, 1997). In contrast, other well-studied surge-type glaciers in Svalbard are underlain solely by soft Mesozoic sedimentary rock (dielectric constant 5-10). However, here, the glacier enters a fjord and its morphology suggests that it may have overridden moraine and glaciomarine sediments, which have lower dielectric constants than metamorphic or igneous rock types, and are readily deformable. Moreover, the bed-profile along the centreline presented by Kotlyakov and Macheret (1987) suggests that a slight overdeepening exists between 1 and 4 km from the terminus, resulting in the glacier emerging into the fjord over an adverse slope and riegel, potentially associated with the outcrop of marble and older moraines at the fjord head.

Consideration of the glacier's geometrical evolution through quiescence provides the best basis for inferences on the changing subglacial conditions of the glacier. Nuth *et al.* (2007, 2010) showed how regional and local glacier mass balances were predominantly negative during Comfortlessbreen's quiescent phase between 1936 and 2005, and coupled to glacier recession in the local region. Indeed, Nuth *et al.* (2007, 2010) demonstrated that thinning of Comfortlessbreen's terminal region was ~1.5-1.8 m a^{-1} for the period 1936 to 1990, and 1-2 m a^{-1} across glaciers in Northwest Spitsbergen between 1966 and 2005. The persistence of these broadly consistent thinning rates since the 1979 geophysical survey data (Kotlyakov and Macheret, 1987) means that ice thickness at the riegel may have decreased from ~150 m to around 100 m by 2006. The contemporary climatic setting in NW Svalbard ensures ice is cold typically to 100 m depth below the glacier surface (Hagen et al, 1993, Bjornsson et al, 1996), which conforms with the observations of the internal reflection horizon at Comfortlessbreen. Consequently, the progressive thinning over the 20th century may have induced the development of a thinner, and increasingly cold terminus, particularly around the riegel. This then could have represented a pinning point which modulated the glacier's flow regime.

A conceptual model of surge evolution

The conceptual model illustrated in Figure 10 is proposed to describe surge initiation, development and termination on Comfortlessbreen:

(1) *Pre-surge*: The earliest observations (1936) of Comfortlessbreen can be drawn from the aerial photographs of its terminal area, as shown in Brandt *et al.* (2007). These show the terminus of the glacier, part of which terminated and calved in tidewater, and part of its braidplain shared with Uvêrsbreen. The terminus was also close to the moraine complex of the forefield (Huddart and Hambrey, 1996), indicating little recession since the Neoglacial maximum of the late 19th and early 20th centuries, despite progressive thinning (Nuth et al., 2007, 2010). This imagery covers as far up-glacier as the Smalfjellbreen confluence, and shows a little-disturbed glacier surface, indicating that the glacier was in quiescent state. During the course of geological observations around Comfortlessbreen and its tributaries during the 1970s and early 1990s (Harland *et al.,* 1993), the glacier surface was easily accessible, longitudinal foliation was the dominant structure, and a supraglacial stream network, which drained into a number of moulins lower down on the glacier, was well

developed. Indeed, there were few attributes to indicate that Comfortlessbreen had previously surged during the residence time of ice within the glacier. These observations suggest either no prior surge history or a minimum length of quiescence before the recent surge of >70 years. During the quiescent or pre-surge phase, ice build-up was significant (more than 60 m) in tributary cirques at the head of the valley and over a large area of the uppermost glacier tongue (Figure 10a). This build-up was less significant in the lower areas of the reservoir zone, extending to slightly below the equilibrium line, and was least pronounced along the eastern margin of the glacier. The thickening rate of the reservoir zone was likely to have been less than the thinning rate in the receiving zone, which in part is a function of the region's low precipitation rates (Melvold & Hagen, 1998). Consequently, the glacier surface steepened over time. Ice velocities decreased throughout quiescence (Blaszczyk *et al.,* 2009; Schneevoight *et al.,* 2012), with only a small area of active flow and crevassing associated with calving.

(2) *Surge initiation:* Ice build-up continued until 2006, at which point an internal threshold was reached, inducing release of ice from the reservoir zone. The polythermal regime of Comfortlessbreen renders the thermal-switch model of Fowler *et al.* (2001) the preferred mechanism by which the surge was initiated. It is likely that the activation wave (the area of thermal switch) propagated down-glacier from an area close to the riegel and overdeepened zone (Figure 10b). This part of the glacier system is where the back stress associated with ice build-up in the glacier's reservoir zone would have been focused, and is the area where pressure-related basal melting would have occurred first. Greater basal ice velocity may have been facilitated through sliding over bedrock or the deformation of a thawed layer of basal sediments, reducing the buttressing of flow by the riegel, and facilitating the advance of the glacier terminus. A similar scenario is described by Flowers *et al.* (2011), whose modelling work emphasises the influence of bedrock topography on the ability of a glacier to surge. This scenario would also have increased stresses on the overlying cold ice, resulting in a greater degree of extending flow, brittle fracture and crevassing, as was witnessed and described for Comfortlessbreen. The subsequent shift in velocity at the terminus would have initiated the drawdown and transfer of ice from the reservoir zone, primarily through the more readily deformable temperate ice at depth. This process would have become quickly amplified as drawdown spread to the thicker, and therefore more predominately temperate, upper reservoir zone.

(3) *Surge propagation:* The drawdown and extension of ice from the reservoir zone (which, vertically, amounted to more than 80 m in places) and its initial transfer towards the receiving zone resulted in extensive crevassing in the higher reaches and profile of the glacier.

However, the rate of ice draw-down and the transfer of mass to the receiving zone were not equal. This was because the propagation of surging ice down-glacier was inhibited by the constriction to ice flow resulting from the bend of the valley tributary confluence (Smalfjellbreen and Nordenfjeldskebreen). This led to the growth of a surge front (Figure 10c). In comparison, the Comfortlessbreen surge front was initially much less pronounced than that of the large bulge on Bakaninbreen (Murray *et al.*, 1998) but represents a much more significant change in geometry than was reported on Monacobreen (Murray *et al.*, 2003b), Fridtjovbreen (Murray *et al.*, 2003a) or Trapridge glacier (Frappê & Clarke, 2007)

The surge front travelled down glacier as a kinematic wave, imparting intense longitudinal compression and a degree of vertical extension on the slower moving ice in its path. A variety of structures, including variable crevasse patterns and thrust-faults, developed in response to this episode of deformation, and pre-existing structures such as longitudinal foliation were heavily modified. The front grew in size through 2008 and 2009, incorporating the less active ice in the receiving zone and eventually reaching 100 m or more in height. By 2009 the surge front had developed to form a gently graded (15-20°), convex, glacier-wide (2.5 km) bulge, which by July had reached the terminus of the glacier. By this time the terminus had steepened to vertical, although retaining a convex profile, disrupted by crevassing.

(4) *Surge cessation*: Once the surge front had reached the terminus of the glacier, it ceased advancing, and the velocity of the glacier declined (Mansell *et al.*, 2012), indicating that the majority of mass-transfer during the surge was concomitant with the passage of the front. According to the Fowler *et al.* (2001) thermal-switch model, surge-termination should occur following the escape of the pressurized water formed at the bed, or through much reduced basal shear stress (Figure 10d). Both of these processes are feasible for Comfortlessbreen when the surge front arrived at the calving zone of the glacier, but definitive evidence of the operation of these processes was not observed during field studies.

When the structural, geometric and dynamic changes the glacier experienced through its surge phase are considered collectively, many similarities between Comfortlessbreen and Bakaninbreen may be identified, although the amount of ice draw-down and mass-transfer, and the rate at which they took place, indicates a surge of greater intensity on Comfortlessbreen. As previously mentioned, the modelling of Fowler *et al.* (2001) predicts an array of surges of variable vigour, and the findings presented above corroborate this aspect of their simulations. Equally, the manifestation of the surge of Comfortlessbreen as a pronounced front offers a degree of validation of the mechanisms and morphology predicted in the model of Fowler *et al.* (2001). Observations of the incomplete surge of Bakaninbreen are the only previous documented evidence of this particular style of surge in Svalbard, although a thermal-switch mechanism has been evoked for Trapridge glacier, Alaska (Frappê & Clarke, 2007). Contemporary observations in Svalbard have indicated widespread thinning in glacier accumulation zones over the last 50 years (James et al., 2012), which may contribute to a continued decline in the number or frequency of surges (Dowdeswell et al., 1995). As highlighted at Trapridge Glacier, the absence of sufficient mass accumulation in the reservoir zone can substantially adjust the progression of a surge cycle (Frappê & Clarke, 2007). Clearly, further detailed interrogation of recent or currently active surge behaviour of Arctic glaciers is needed to constrain future surge dynamics and their association with regional ice mass decline.

8. Conclusions

Through the derivation and examination of DEMs of the surface of Comfortlessbreen and the extensive documentation of structural features present at different stages of the glacier's recent surge, the geometric and structural evolution of the glacier has been reconstructed. This analysis reveals that contrasting flow regimes existed during quiescent and surge-phase flow. Quiescence was typified by minimal, creep-dominated flow with longitudinal foliation the pervasive feature at the glacier's surface. Crevassing was restricted to the terminal calving zone. Surge-phase structures support the inference that block-flow facilitated ice-transfer from the reservoir zone to the receiving zone of the glacier. Compressional features dominate the receiving zone of the glacier later in the surge. Towards the terminal zone of the glacier, structures developed which may be attributable to the passage of a surge front later in the active phase.

DEM analysis shows similarities between the evolving geometry of Comfortlessbreen and other surge-type glaciers in Svalbard. Substantial ice-surface lowering occurred in the reservoir zone (up to 80 m) with vertical ice-surface elevation increases reaching 100 m in the receiving zone over 4 years. The height of the suspected surge front resembles previously reported examples, reinforcing the validity of the proposed model of development presented here.

Lastly, the collation of the results from this and earlier investigations facilitates the development of a conceptual model to describe the surge. The surge of Comfortlessbreen was manifested as a pronounced front because of the flow-restrictive nature of the valley configuration and the impact of tributaries. This led to delayed transfer of ice from the reservoir zone and the growth of a gently graded bulge that migrated down-glacier. Here, the role of a subglacial riegel is invoked as a potential cause for a thermal-switch surge mechanism. The surge terminated soon after this front reached the terminus, presumably as pressurized water escaped from the bed and as basal shear stress diminished. Continued investigation into the interplay between contemporary climate, thermal regime and basal topography is necessary in order to better constrain Arctic glacier dynamics.

Acknowledgements

The authors thank Professor Doug Benn for comments on an early draft of this manuscript. Detailed reviews from Dr Phil Porter and an anonymous referee were greatly appreciated. MJH acknowledges the support of the European Centre for Arctic Environmental Research in Ny-Ålesund (Grant no. ARCFAC-026129-2008-47) and the logistical support of the French-German Arctic Research Base (AWIPEV), led by Dr Marcus Schumacher. We are grateful for the help of the Norwegian Polar Institute, particularly Harald Faste Aas, for providing access to their aerial photo archive and 1990 DEM.

References

Adhikari S, Marshall SJ. 2012. Parameterization of lateral drag in flowline models of glacier dynamics. *Journal of Glaciology* **58** (212): 1119-1132.

Bamber JL. 1989. Ice/bed interface and englacial properties of Svalbard ice masses deduced from airborne radio echo-sounding data. *Journal of Glaciology* **35**(119): 30-37.

Barrand NE, Murray T, James TD, Barr SL, Mills JP. 2009. Optimizing photogrammetric DEMs for glacier volume change assessment using laser-scanning derived ground-control points. *Journal of Glaciology* **55** (189): 106-115.

Barrand NE, James TD, Murray T. 2010. Spatio-temporal variability in elevation changes of two high-arctic valley glaciers. *Journal of Glaciology* **56** (199): 771-770.

Bevington A, Copland L. 2014. Characteristics of the last five surges of Lowell Glacier, Yukon, Canada, since 1948. *Journal of glaciology* **60** (219): 113-123.

Björnsson H, Gjessing Y, Hamran S-E, Hagen JO, Liestøl O, Pálsson F, Erlingsson B. 1996. The thermal regime of sub-polar glaciers mapped by multi-frequency radio-echo sounding. *Journal of Glaciology* **42** (140): 23-32.

736 Blaszczyk M, Jania JA, Hagen JO. Tidewater glaciers of Svalbard: Recent changes and
737 estimates of calving fluxes. *Polish Polar Research* **30** (3): 85-142.

738 Brandt O, Langley K, Kohler J, Hamran SK. 2007. Detection of buried ice and sediment
739 layers in permafrost using multi-frequency ground penetrating radar: A case examination
740 on Svalbard. *Remote sensing of environment* **111**: 212-227.

741 Clarke G. 1976. Thermal regulation of glacier surging. *Journal of Glaciology* **16** (74): P231-
742 250.

743 Clarke G, Collins SG, Thompson DE. 1984. Flow, thermal structure and subglacial conditions
744 of a surge-type glacier. *Canadian Journal of Earth Sciences* **21**(2): 232-240.

745 Comiso J. C., and Hall, D. K. 2014. Climate trends in the Arctic as observed from space.
746 Wiley Interdisciplinary Reviews: Climate Change, **5**(3): 389-409.

747 Copland L, Sylvestre T., Bishop M., Shroder JF., Seong YB., Owen LA., Bush A., Kamp U.
748 2011. Expanded and recently increased glacier surging in the Karakoram. *Arctic,*
749 *Antarctic and Alpine Research* **43** (4): 503-516.

750 Croot DG. 1988. Glaciotectonics and surging glaciers: a correlation based on
751 Vestspitsbergen, Svalbard, Norway. *In* Croot, D.G., ed. *Glaciotectonics: forms and*
752 *processes*. Rotterdam, A.A. Balkema, 49-61.

753 De Paoli L, Flowers G. 2009. Dynamics of a small surge-type glacier using one-dimensional
754 geophysical inversion. *Journal of Glaciology* **55** (194): 1101-1113.

755 Dowdeswell JA, Hamilton GS, and Hagen JO. 1991. The duration of the active phase on
756 surge-type glaciers: contrasts between Svalbard and other regions. *Journal of Glaciology*
757 **37**(127): 388-400.

758 Dowdeswell JA, Hodgkins R, Nuttall A-M, Hagen JO, Hamilton GS. 1995. Mass balance
759 change as a control on the frequency and occurrence of glacier surges in Svalbard,
760 Norwegian High Arctic. *Geophysical Research Letters* **22**(21): 2909-2912.

Dowdeswell JA, Hambrey MJ. 2002. *Islands of the Arctic*. Cambridge University Press. Cambridge. 280 pages.

Dowdeswell JA, Benham TJ. 2003. A surge of Perseibreen, Svalbard, examined using aerial photography and ASTER high resolution satellite imagery. *Polar research* **22** (2): 373-383.

Eisen O, Harrison W.D and Raymond CF. 2001. The surges of Variegated Glacier, Alaska, USA, and their connection to climate and mass balance. *Journal of Glaciology*, **47** (158): 351-358.

Eisen O, Harrison WD, Raymond CF, Echelmeyer KA, Bender GA, Gorda JLD. 2005. Variegated Glacier, Alaska, USA: a century of surges. *Journal of Glaciology* **51** (174): 1-9.

Flowers G, Rour N, Pimentel S, Schoof CG. 2011. Present dynamics and future prognosis of a slowly surging glacier. *The cryosphere* **5:** 299-313.

Fowler AC, Murray T, Ng FSL. 2001. Thermally controlled glacier surging. *Journal of Glaciology* **47**: 527-538.

Frappé TP, Clarke GKC. 2007. Slow surge of Trapridge Glacier, Yukon Territory, Canada. *Journal of geophysical Research* **112** (F3) DOI: 10.1029/2006JF000607.

Glasser NF, Hambrey MJ, Crawford K, Bennett MR, Huddart D. 1998. The structural glaciology of Kongsvegen, Svalbard and its role in landform genesis. *Journal of Glaciol*ogy **44**(146): 136-148.

Glasser NF, Scambos TA. 2008. A structural glaciological analysis of the Larsen B ice-shelf collapse. *Journal of Glaciol*ogy **54** (184): 3-16.

Goodsell B, Hambrey MJ, Glasser NF, Nienow P, Mair D . 2005. The structural glaciology of a temperate valley glacier: Haut Glacier d'Arolla, Valais, Switzerland. *Arctic, Antarctic and Alpine Research* **37** (2): 218-232.

Grant K. L., Stokes C. R., & Evans I. S. 2009. Identification and characteristics of surge-type glaciers on Novaya Zemlya, Russian Arctic. *Journal of Glaciology*, **55**(194): 960-972.

Hagen JO. 1987. Glacier surge at Usherbreen, Svalbard. *Polar Research* **5**(2): 239-252.

Hagen JO, Sætrang A. 1991. Radio-echo soundings of subpolar glaciers with low-frequency radar. *Polar Research* **9**(1): 99-107.

Hagen JO, Eiken T, Kohler J, Melvold K. 2005. Geometry changes on Svalbard glaciers: mass-balance or dynamic response? *Annals of Glaciology* **42**: 255-261.

Hagen JO, Liestøl O, Roland E, Jorgense T. 1993. *Glacier Atlas of Svalbard and Jan Mayen. Norsk Polarinstitutts meddelelser*. **129.**

Hambrey MJ, Dowdeswell JA. 1997. Structural evolution of a surge-type glacier: Hessbreen, Svalbard. *Annals of Glaciology* **24**: 375-381.

Hambrey MJ, Huddart D. 1995. Englacial and proglacial glaciotectonic processes at the snout of a thermally complex glacier in Svalbard. *Journal of Quaternary Science* **10**(4): 313-326.

Hambrey MJ, Dowdeswell JA, Murray T, Porter PR. 1996. Thrusting and debris-entrainment in a surging glacier, Bakaninbreen, Svalbard. *Annals of Glaciology* **22**: 241-248.

Hambrey MJ, Lawson WJ. 2000. Structural styles and deformation fields in glaciers: a review. *In* Maltman, A.J., Hubbard, B. and Hambrey, M. J. (eds.) Deformation of Glacial Materials, Geological Society, London, Special Publications. **176**: 59-83.

Hambrey MJ, Waddams P. 1981. Deformed stones of varied lithology in Late Precambrian tillites, western Spitsbergen. *Journal of the Geoogical society, London* **138**: 445-453.

Hamran S-E, Aarholt E, Hagen JO, Mo P. 1996. Estimation of relative water content in a subpolar glacier using surface-penetration radar. *Journal of Glaciology* **42** (142): 533-537.

Harland WB.1997. *The Geology of Svalbard*. Geological Society of London, Memoir No. 17.

Harland WB, Hambrey MJ, Waddams P. 1993. *Vendian Geology of Svalbard*. Norsk. Polarinstitutt Skrifter **193**

Herzfeld UC, Clarke G, Mayer H, Greve R. 2004. Derivation of deformation characteristics in fast-moving glaciers. *Computers and Geosciences* **30**: 291-302.

Holt TO, Glasser NF, Quincey DJ, Siegfried MR. 2012. Speedup and fracturing of George VI Ice Shelf, Antarctic Peninsula. *The Cryosphere* **7**: 797-816, DOI: 10.5194/tc-7-797-2013

Hooke R LeB, Hudleston P. 1978. Origin of foliation in glaciers. *Journal of Glaciology* **20**: 285-299.

Hodgkins R, Fox A, Nuttall A-M. 2007. Geometry change between 1990 and 2003 at Finsterwalderbreen, a Svalbard surge-type glacier, from GPS profiling. *Annals of Glaciology* **46**: 131-135.

Huddart D, Hambrey MJ. 1996 Sedimentary and tectonic development of a high-arctic, thrust-moraine complex: Comfortlessbreen, Svalbard. *Boreas* **25**(4): 227-243.

James TD, Murray T, Barrand NE, Sykes SJ, Fox AJ, King MA. 2012. Observations of widespread accelerated thinning in the upper reaches of Svalbard glaciers. *The Cryosphere Discussions*. DOI:10.5194/tcd-6-1085-2012.

Jennings S. J., Hambrey M. J. and Glasser N. F. 2014. Ice flow-unit influence on glacier structure, debris entrainment and transport. *Earth Surface Processes and Landforms*, **39**(10): 1279-1292.

Jiskoot H, Boyle P, Murray T. 1998. The incidence of glacier surging in Svalbard: evidence from multivariate statistics. *Computers and Geosciences* **24**(4): 387-399.

Jiskoot H, Murray T, Boyle PJ. 2000. Controls on the distribution of surge-type glaciers in Svalbard, *Journal of Glaciology* **46**(154): 412-422.

Kamb B, Raymond CF, Harrison WD, Engelhardt H, Echelmeyer KA, Humphrey N, Brugman MM, Pfeffer T. Glacier surge mechanism: 1982-1983 surge of Variegated Glacier, Alaska. *Science* **227** (4686): 469-479.

Kohler J. Nordli Ø, Brandt O, Isaksson E, Pohjola V, Martma T, Aas HF. 2003. Svalbard temperature and precipitation, late 19th century to the present. *Final Report on ACIA-Funded Project*. Norsk Polarinstitutt, Oslo, Norway, 21pages.

Kohler J, James TD, Murray T, Nuth C, Brandt O, Barrand NE, Aas HF. 2007. Acceleration in thinning rate on western Svalbard glaciers. *Geophysical Research Letters* **34** DOI: 10.1029/2007GL030681.

Kotlyakov VM, Macheret YY. 1987. Radio echo sounding of sub-polar glaciers in Svalbard: Some problems and results of soviet studies. *Annals of Glaciology* **9**: 151-159.

Lavrentiev I. 2007. Fridtjovbreen changes in 20th century from remote sensing data. *In*. The dynamics and mass buddget of Arctic glaciers, extended abstracts. GLACIODYN workshop 2007; 61-63.

Lefauconnier B, Hagen JO. 1991: Surging and calving glaciers in eastern Svalbard. *Norsk Polarinstitutt. Medelelser* **116**.

Liestøl O. 1969. Glacier surges in West Spitsbergen. *Canadian Journal of Earth Science*, **6**: 895-897.

Mansell D, Luckman A, Murray T. 2012. Dynamics of tidewater surge-type glaciers in northwest Svalbard. *Journal of Glaciol*ogy **58** (207): 110-119.

Meier MF, Post AS. 1969. What are glacier surges? *Canadian Journal of Earth Science*. **6:** 807-817.

Melvold K, Hagen JO. 1998. Evolution of a surge-type glacier in its quiescent phase: Kongsvegen, Spitsbergen, 1964–95. *Journal of Glaciol*ogy **44**(147): 394–404.

Murray T, Dowdeswell JA, Drewry DJ, Frearson I. 1998. Geometric evolution and ice dynamics during a surge of Bakaninbreen, Svalbard. *Journal of Glaciol*ogy **44** (187): 263-273.

Murray T, Stuart GW, Miller PJ, Woodward J, Smith AM, Porter PR, Jiskoot H. 2000. Glacier surge propagation by thermal evolution at the bed, *Journal of Geophysical Research*, **105**(B6): 13491-13507.

Murray T, Luckman A, Strozzi T, Nuttall A-M. 2003a. The initiation of glacier surging at Fridtjovbreen, Svalbard. *Annals of Glaciology* **36**(1) : 110-116.

Murray T, Strozzi T, Luckman A, Jiskoot H, Christakos, P. 2003b. Is there a single surge mechanism? Contrasts in dynamics between glacier surges in Svalbard and other regions. *Journal of Geophysical research*, **108**. DOI:10.1029/2002JB001906.

Nolan M. 2003. The 'Galloping Glacier' trots: decadal-scale speed oscillations within the quiescent phase. *Annals of Glaciol*ogy **36**: 7-13.

Nuth C, Kohler J, Aas HF, Brandt O, and Hagen JO. 2007. Glacier geometry and elevation changes on Svalbard (1936-90): a baseline dataset. *Annals of Glaciol*ogy **46** (8): 1-11.

Nuth C, Moholdt G, Kohler J, Hagen JO, Kääb A . 2010. Svalbard glacier elevation changes and contribution to sea level rise. *Geophysical Research Letters*, **115,** F01008. DOI: 10.1029/2008JF001223.

Pimentel S, Flowers GE, Schoof CG. 2010. A hydrologically coupled higher-order flow-band model of ice dynamics with a Coulomb friction sliding law. *Journal of Geophysical Research* **115**: DOI:10.1029/2009JF001621

Raymond CF. 1987. How do glaciers surge? A review. *Journal of Geophysical Research*., **92**: 9121-9134.

Rolstad C, Amlien J, Hagen JO, Lunden B. 1997. Visible and near-infrared digital images for the determination of ice velocities and surface elevation during a surge on Osbornebreen, a tidewater glacier in Svalbard. *Annals of Glaciology* **24**: 255-261.

Schneevoight N.J, Sund M, Bogren W and Kääb A. 2012. Glacier displacement on Comfortlessbreen, Svalbard, using 2-pass differential SAR interferometry (DInSAR) with a digital elevation model. *Polar Record* **48** (244): 17-25.

Sharp MJ, Ananicheva M, Arendt A, Hagen J-O, Hock R, Josberger E, Moore D, Pfeffer T, and Wolken G.J. 2011. "Mountain Glaciers and Ice Caps". In: AMAP, 2011. Snow, Water, Ice and Permafrost in the Arctic (SWIPA). Arctic Monitoring and Assessment Program (AMAP), Oslo. 7-1 - 7-61.

Sund M, Eiken T, Hagen JO, Kääb A. 2009. Svalbard surge dynamics derived from geometric changes*. Annals of Glaciol*ogy **50**(52): 50-60.

Sund M, Eiken T. 2010. Recent surges on Blomstrandbreen, Comfortlessbreen and Nathorstbreen, Svalbard. *Journal of Glaciology*, **56**(195): 182-184.

Woodward J, Murray T, McCaig A. 2002. Formation and reorientation of structures in the surge-type glacier Kongsvegen, Svalbard. *Journal of Quaternary Science* **17**(3): 201-209.

Table 1. Aerial photographs used in structural mapping and DEM extraction.

Scene ID	Date of acquisition
s2009_13822_00648	July/August 2009
s2009_13822_00647	July/August 2009
s2009_13822_00646	July/August 2009
s2009_13822_00209	July/August 2009
s2009_13822_00208	July/August 2009
s2009_13822_00135	July/August 2009
s2009_13822_00136	July/August 2009
s2009_13822_00137	July/August 2009
s2009_13822_00138	July/August 2009
s2008_13658_00317	July 2008
s2008_13658_00316	July 2008
s2008_13658_00315	July 2008
s2008_13658_00314	July 2008
s2008_13658_00313	July 2008
s2008_13658_00312	July 2008
s2008_13658_00311	July 2008
s2008_13658_00324	July 2008
s2008_13658_00325	July 2008
s2008_13658_00326	July 2008
S90_6522	August 1990
S90_6523	August 1990
S90_6524	August 1990
S90_6764	August 1990
S90_6763	August 1990
S90_6563	August 1990
S90_6525	August 1990

Table 2. Summary of geometric changes experienced by selected tidewater terminating surge-type glacier in Svalbard (polythermal) and Alaska (temperate). Where elevation data from the surge front are absent, no surge front was reported to have developed on those respective glaciers.

Glacier name	Lowering of reservoir zone (m)	Thickening of receiving zone (m)	Maximum surge front height (m)	Source
Bakaninbreen (Svalbard)	-15	+70	+70	Murray *et al.* (1998)
Fridtjovbreen (Svalbard)	-180	+60	-	Lavrentiev (2007)
Perseibreen (Svalbard)	-120	+140	-	Sund *et al.* (2009)
Osbornebreen (Svalbard)	-100	+100	-	Rolstad *et al.* (1997)
Comfortlessbreen (Svalbard)	-80	+100	+100	-
Variegated (Alaska)	-40	+110	+100	Raymond (1987)
Trapridge (Alaska)	-10	-10	-	Frappê & Clarke, (2007)

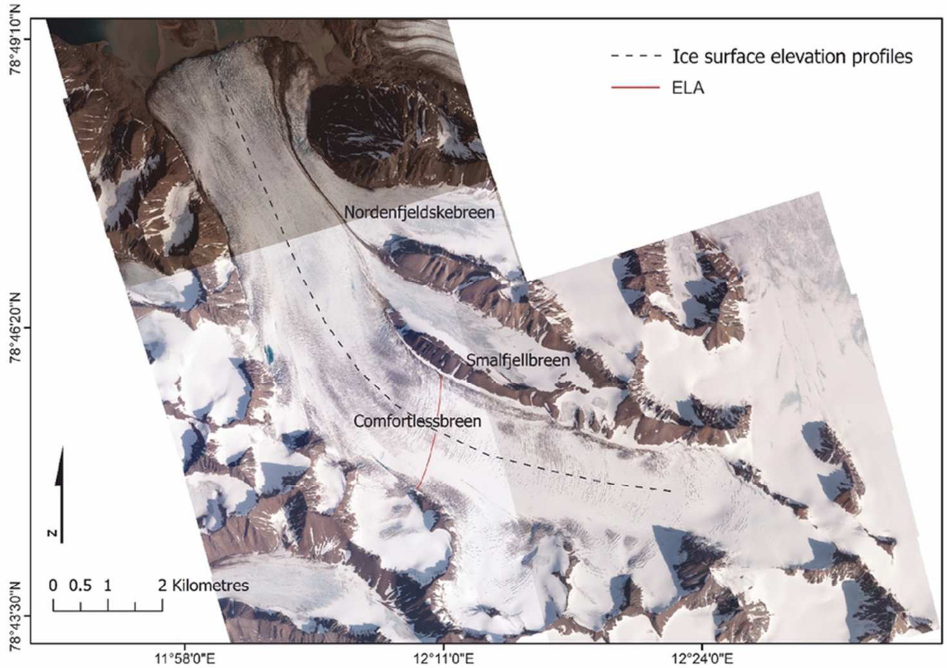

Figure 1. Comfortlessbreen, illustrating the coverage of Norsk Polarinstitutt's aerial photography used in this study. Imagery shown was taken in August 2009. The marked equilibrium line altitude (ELA) is approximate and marks summer snowline extent in 1990 aerial photographs.
78x55mm (300 x 300 DPI)

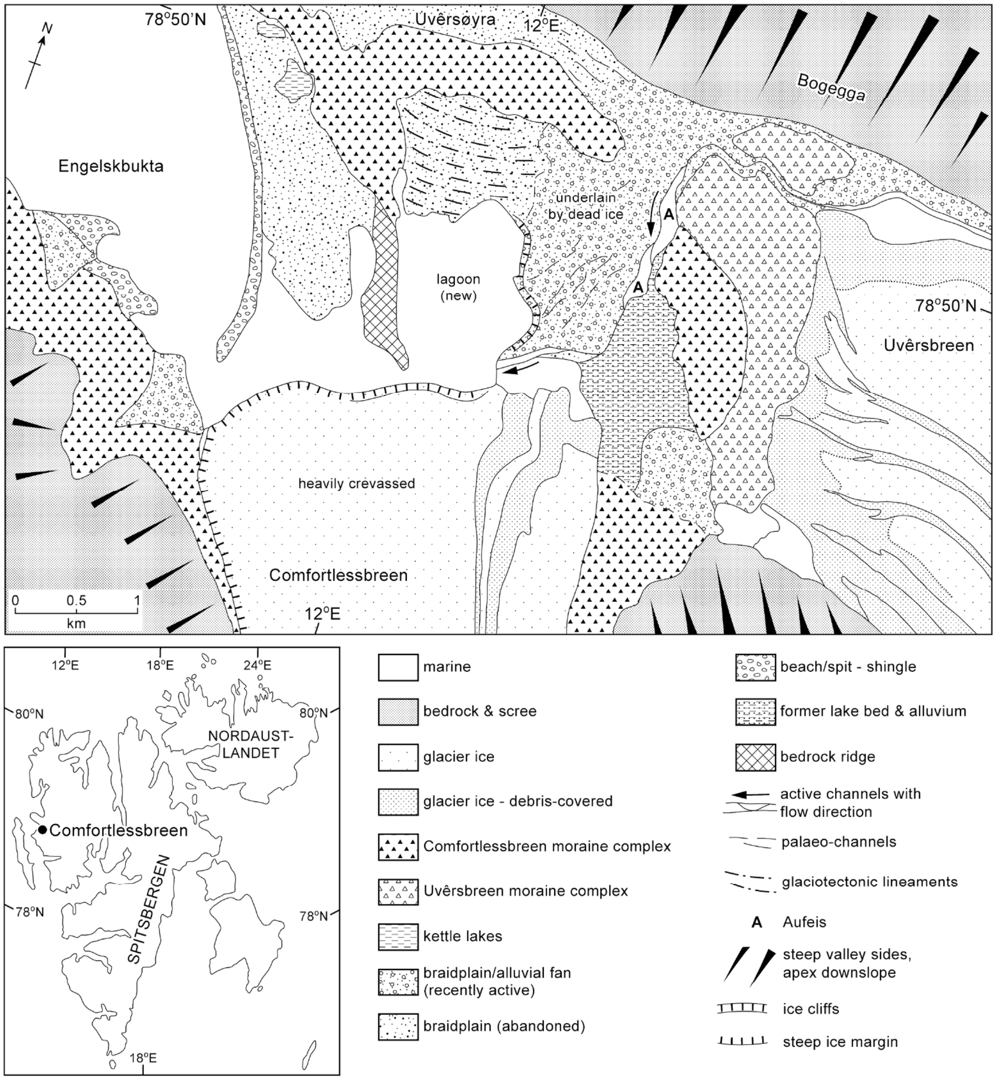

Figure 2. Geomorphological map of terminal region of Comfortlessbreen and adjacent Uvêrsbreen, based on a Quickbird image dated 28 August 2008, with additional detail from earlier aerial photographs and a map of Huddart and Hambrey (1995).
204x220mm (300 x 300 DPI)

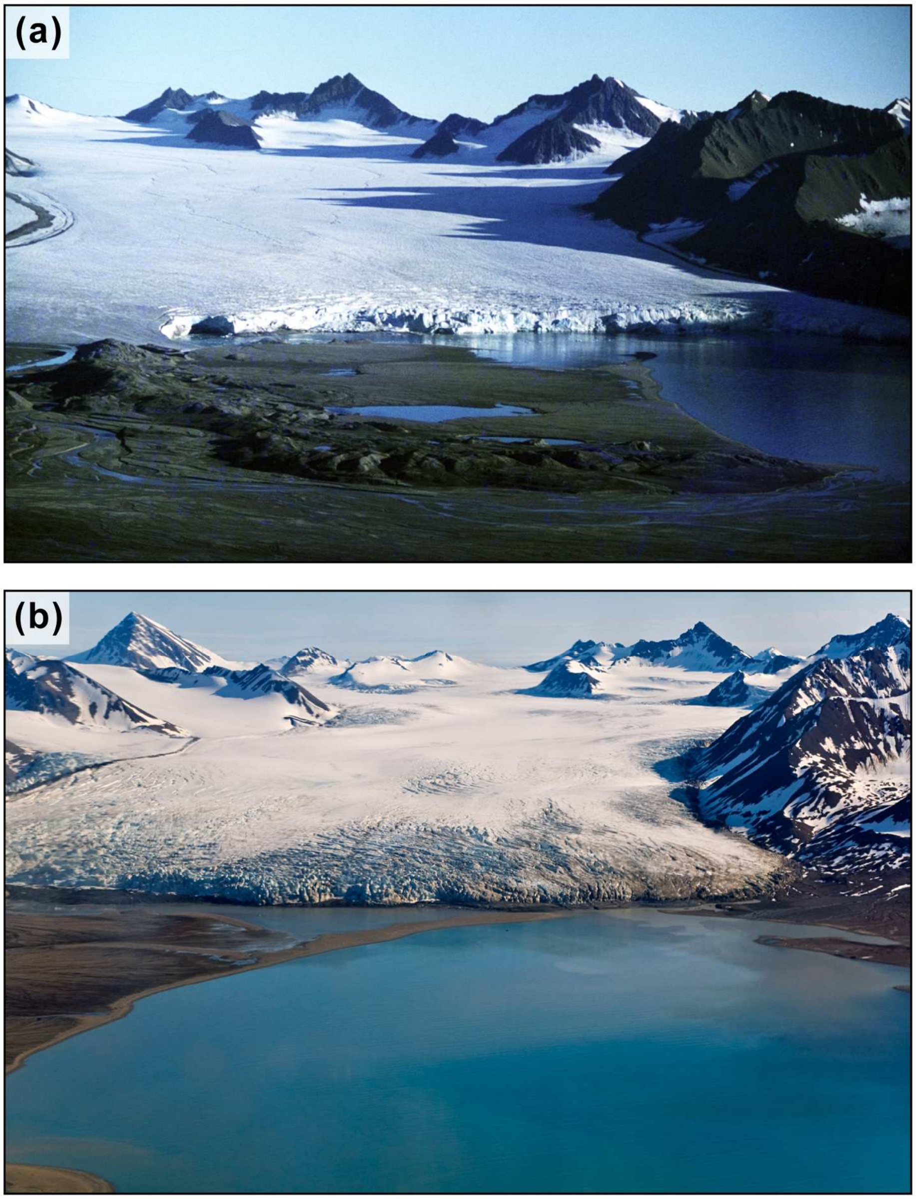

Figure 3. Contrasting views of the terminus of Comfortlessbreen in (a) August 1978 when the glacier was slowly receding (telephoto from surrounding hills) and on (b) 12 July 2009 when the glacier was in surge-mode (oblique aerial photograph).
162x211mm (300 x 300 DPI)

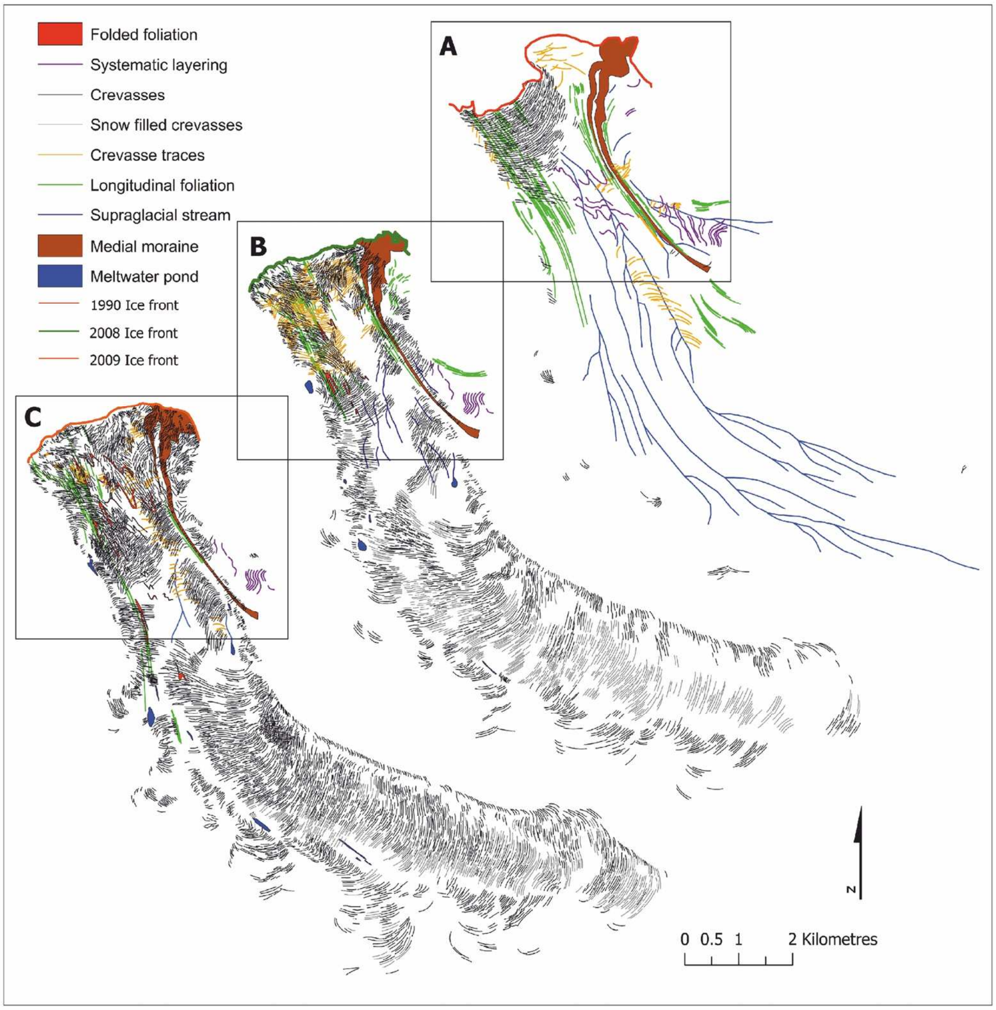

Figure 4. Structural maps of features present at the surface of Comfortlessbreen from (A) quiescence (1990) into the latter stages of surge (2008-B, 2009-C). Snow-bridged crevasses have been identified through standard image enhancement techniques and contrast stretching. Systematic layering on Nordenfjeldskebreen has also been mapped (to the east). Approximately 700 m of ice front advance occurred between 1990 and 2009.
146x149mm (300 x 300 DPI)

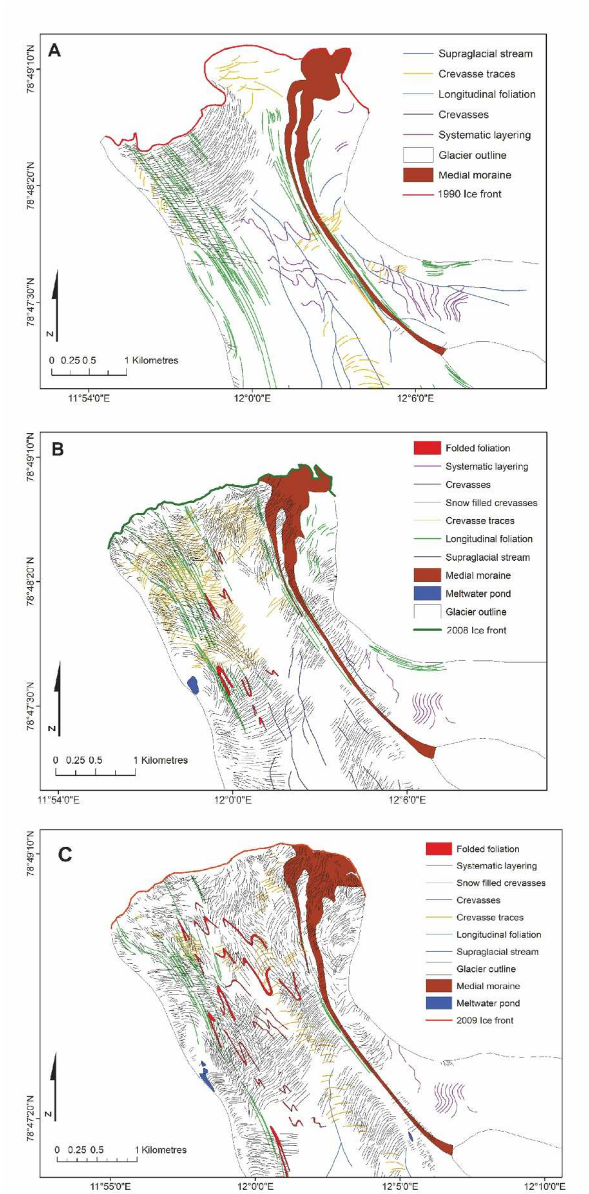

Figure 5. Structural maps of the terminal area of Comfortlessbreen from A) 1990, B) 2008 and C) 2009.
144x290mm (300 x 300 DPI)

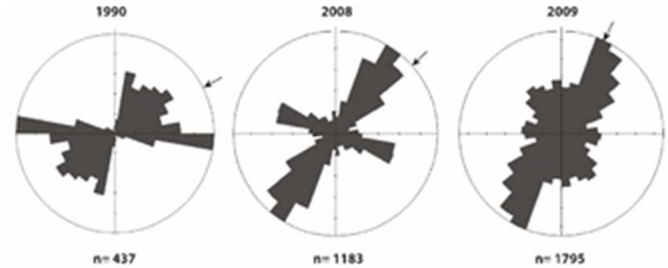

Figure 6. Rose diagrams showing crevasse orientation over the lower reaches of Comfortlessbreen (downglacier of Nordenfjeldskebreen confluence) in, from left to right, late quiescence, mid-surge and the later stages of surge. Arrows mark mean orientation.
28x11mm (300 x 300 DPI)

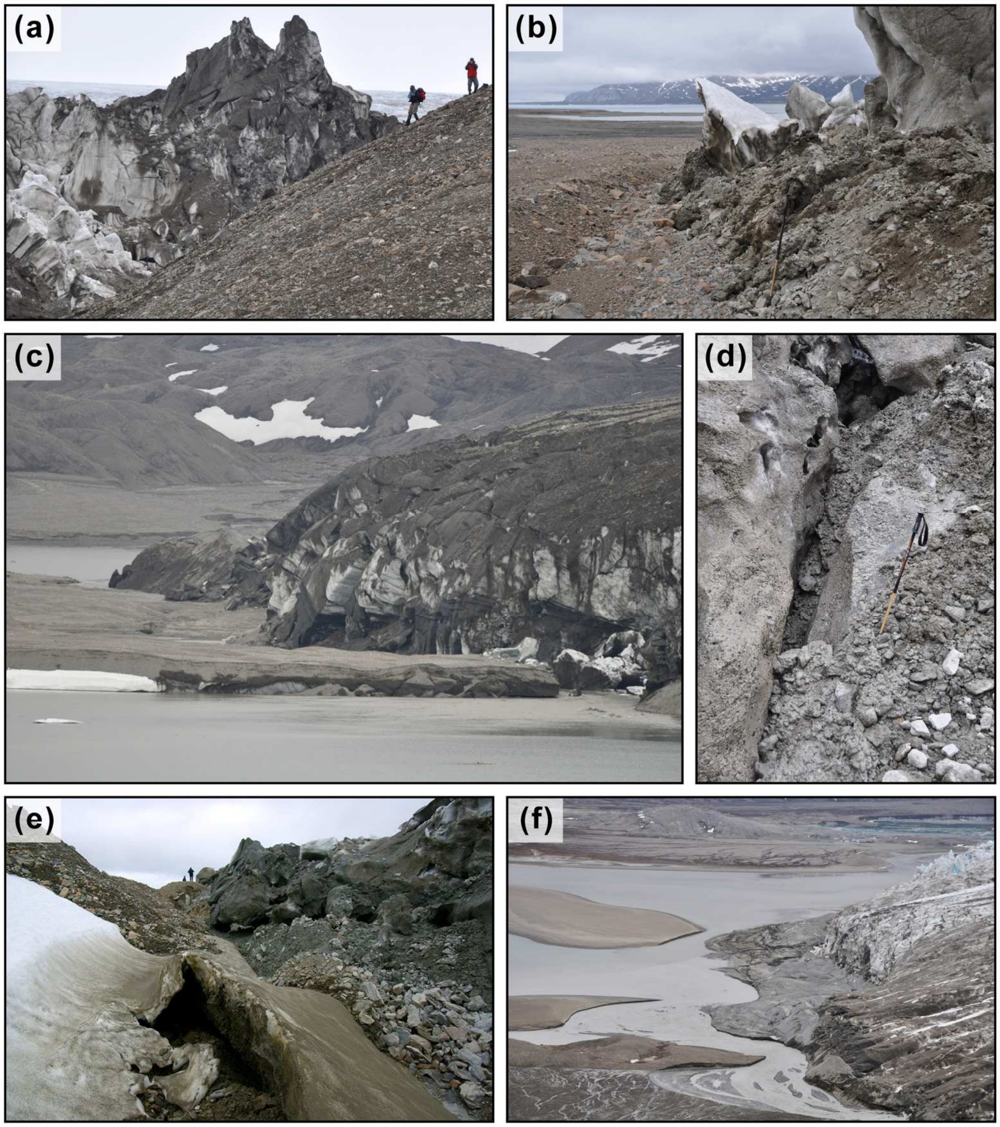

Figure 7. Ice-marginal features of Comfortlessbreen during surge in July 2009. (a) Shear zone with heavy crevassing and séracs at left margin. (b) Thrust wedges of sandy gravel, derived from lateral moraine material, left margin near snout. (c) Debris-draped ice margin with thrusts delivering material from the bed, mid-front of glacier. (d) A rare basal crevasse, filled with diamicton (originally subglacial till), left-lateral margin. (e) Folding of a snow bank as the glacier impinges on the left-lateral moraine. (f) Ridges of glaciomarine mud, pushed up in front of the glacier as it surges; note the lack of ice-contact with marine waters resulting from the formation of these intervening ridges, and enhanced tidal erosion of the landward side of the spit.
161x182mm (300 x 300 DPI)

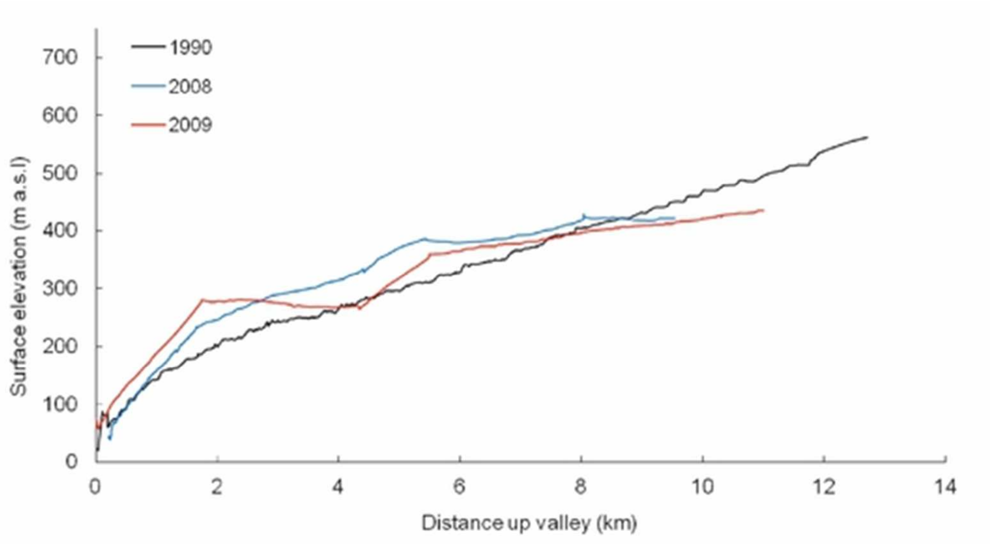

Figure 8. Longitudinal surface elevation profiles taken from DEMs of the glacier surface for 1990, 2008 and 2009 respectively. All profiles are taken from the glacier terminus up-glacier.
45x24mm (300 x 300 DPI)

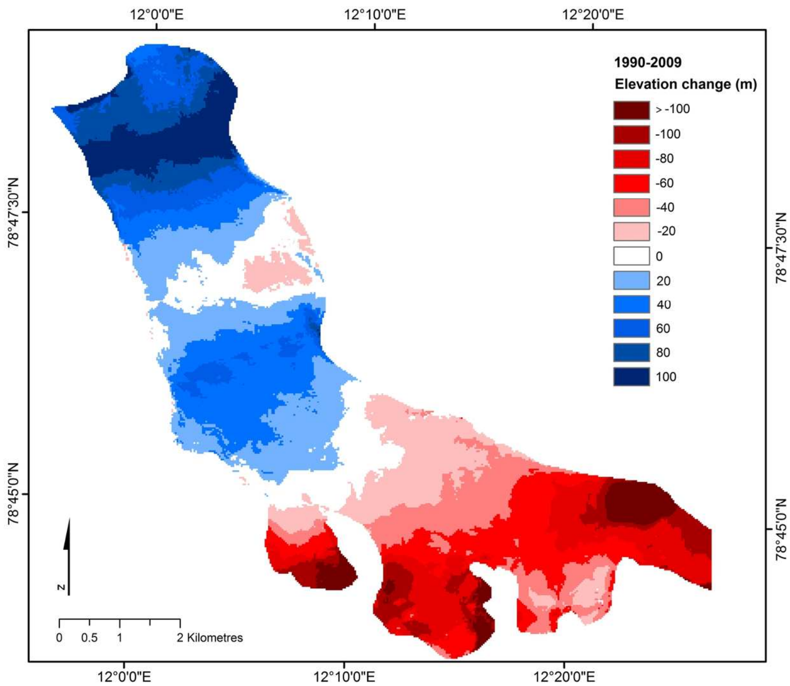

Figure 9. Elevation changes over the surface of Comfortlessbreen derived through DEM-differencing from late quiescence (1990) through to the later stages of the surge (2009).
168x118mm (300 x 300 DPI)

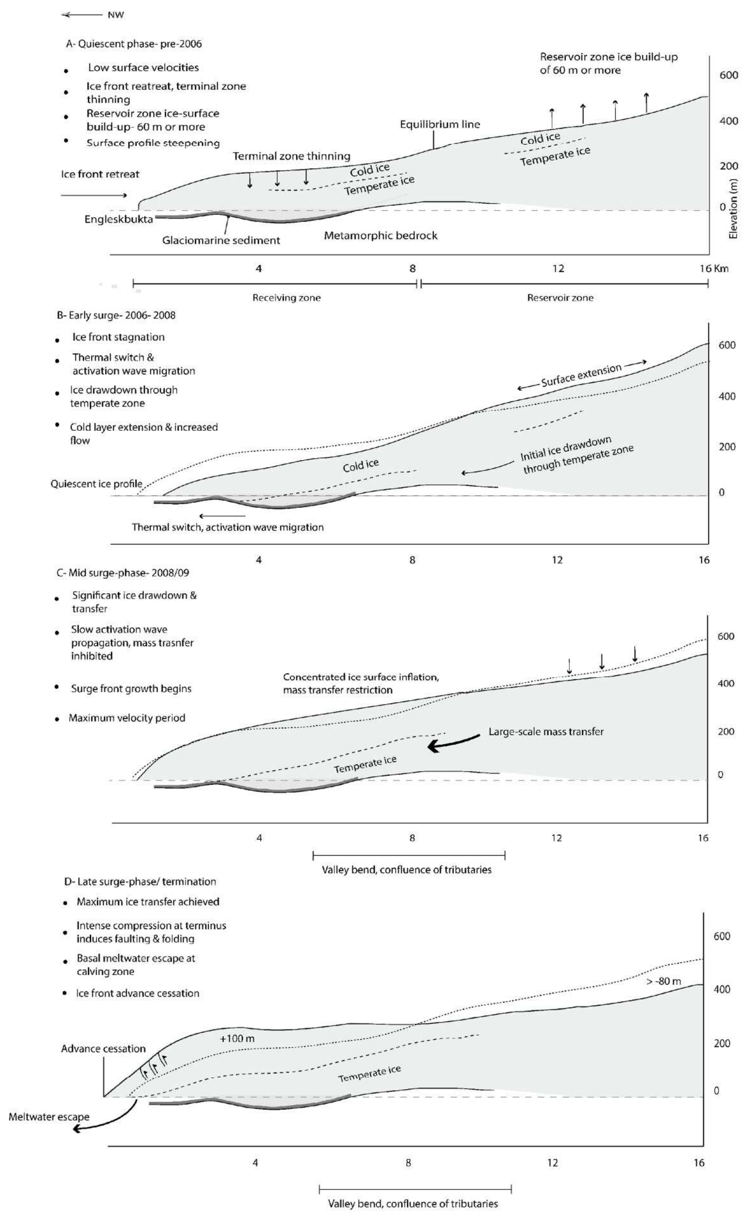

Figure 10. Conceptual model to describe the evolution of the surge of Comfortlessbreen.
151x247mm (300 x 300 DPI)